JOURNAL OF GEOPHYSICAL RESEARCH, VOL. 104, NO. D24, PAGES 31,753–31,762, DECEMBER 27, 1999

Particle size distribution retrieval from multispectral optical depth: Influences of particle nonsphericity and refractive index

Yangang Liu,[1] W. Patrick Arnott, and John Hallett

Desert Research Institute, Atmospheric Sciences Center, Reno, Nevada

Abstract. Retrieval of size distributions from multispectral optical depth measurements requires solution of an ill-posed inverse problem. The ill-posedness causes problems such as solution ambiguity. Size distribution retrieval becomes more complicated in the presence of nonspherical particles and/or refractive index errors. A new retrieval algorithm is first developed which allows for both smoothing and nonnegativity constraint along with the L-curve method for choosing the Lagrange multiplier that controls the degree of the imposed smoothing. This new algorithm is compared to an iterative algorithm and the method of truncated singular value decomposition, demonstrating that the new algorithm outperforms the other two. With the new algorithm to perform the size distribution retrieval and with the T-matrix method to calculate optical depth for a given cloud consisting of randomly oriented finite circular cylinders, the influence of particle nonsphericity on the size distribution retrieval is investigated by use of the Mie theory for spheres as well as the anomalous diffraction theory for cylinders. The results show that spurious particles and even spurious particle modes occur for both approximations. The effect of refractive index errors are also investigated, showing that even a small perturbation of refractive indices can cause serious distortions of retrieved size distributions. A further examination reveals that either applying an approximate light-scattering theory (Mie theory or anomalous diffraction theory) to nonspherical particles or using incorrect refractive indices results in systematic errors in the model which in turn conspire with the ill-posedness inherent in the retrieval to cause the distortions of retrieved size distributions. The retrieval process essentially transforms the model error into the error in retrieved size distribution, yet improves the agreement between true and retrieved optical depth.

1. Introduction

Various properties (e.g., dynamical, optical, electrical, and chemical) of atmospheric particles depend on particle size. Number distribution of particles with respect to size (size distribution) is a fundamental subject in aerosol and cloud physics [*Pruppacher and Klett*, 1978]. Its importance has been increasingly recognized with the concern over the effects of aerosols and clouds on radiation transfer and climate. Instrumentation for measuring sizing distributions has continued to occupy a prominent position among problems in atmospheric sciences. Although significant advances have been made in the past decades [*Deirmendjian*, 1980; *Knollenberg*, 1981; *Kerker*, 1997], a serious problem inherent in the particle-sizing instrumentation remains: the associated mathematical problem that needs to be solved to obtain size distributions is ill-posed in the sense that measured size distributions are highly sensitive to errors in measured signals and calculated scattering properties. This is particularly true for indirect retrieval [*Twomey*, 1977]. In fact, development of methods for dealing with the ill-posedness to obtain a useful solution is still an active area of research [*Hansen*, 1998].

On the other hand, atmospheric particles such as aerosol particles and ice crystals are often nonspherical. For a cloud of nonspherical particles, optical properties such as extinction depend on particle shape and orientation in addition to size distribution and refractive index. There is abundant experimental and theoretical evidence that the Mie theory is, in general, inadequate to approximate scattering properties of nonspherical particles [*Fu and Liou*, 1993; *Mishchenko et al*., 1996; *Yang et al*., 1997]. The discrepancy between in situ measurements of crystal size and retrieved crystal size from infrared radiometric measurements has led to a debate over the existence of small crystals and their role in radiation transfer. It has been argued that the existence of small crystals may be caused by the inappropriate treatment of nonspherical scattering in the approximation of equivalent spheres [*Mitchell and Arnott*, 1994; *Baran et al*., 1998]. Particle nonsphericity is expected to have more significant effects on the size distribution retrieval because of the inherent ill-posedness. It is anticipated that the Mie-theory-based retrieval may produce spurious size distributions in the presence of nonspherical particles. In a recent numerical experiment we inverted ice crystal size distributions from multispectral extinction measurements in laboratory ice clouds by applying the Mie theory to ice spheres, and the extinction calculated from thus retrieved size distribution of ice spheres closely agreed with the measured value [*Arnott et al*., 1996]. The

[1]Now at Environmental Chemistry Division, Brookhaven Research Laboratory, Upton, New York.

Copyright 1999 by the American Geophysical Union.

Paper number 1998JD200122.
0148-0227/99/1998JD200122$09.00

results of this numerical study imply that the incorrect representation of particle shape may be transformed into an incorrect size distribution of nonspherical particles, without much loss of agreement between modeled and measured radiative properties. Such mutual "contamination" between particle shape and size questions the reliability of any size (distribution) measurements when nonspherical particles are present.

The anomalous diffraction theory (ADT) is another commonly used approximation to scattering by nonspherical particles. Some argue that ADT may be better than the Mie theory for approximating light scattering by nonspherical particles [*Baran et al*., 1998]. Recently, we [*Liu et al*., 1998] developed an exact ADT for finite cylinders and demonstrated that ADT tends to work better with deviation of particle shape from spheres only for specific cases, for example, in the Christiansen bands where the real part of the refractive index approaches unity and/or at the wavenumber where relative absorption is strong. Because size distribution retrieval uses a wide range of all the wavenumbers, the ADT performance in the retrieval requires further analysis.

Another unrealistic assumption that has been widely used in previous studies of size distribution retrieval is that refractive indices are accurately known. In reality, our knowledge of refractive index, however, is uncertain. For aerosols, refractive index is essentially unknown since they are mixtures of a variety of aerosol types and chemical composition [*Penner et al*., 1994]. Uncertainties even exist for the well-documented water refractive index [*Arnott et al*., 1997]. Just as with applying the Mie theory to nonspherical particles, using incorrect refractive indices are expected to distort the retrieved size distribution.

Because of the difficulties in treating the ill-posedness associated with retrieval problems and in calculating light scattering, only a few studies have been published to address the influences of particle nonsphericity and refractive index on size distribution retrieval [*Welch et al.*, 1981]. This is particularly true for the effect of particle nonsphericity.

This paper is devoted to the development of retrieval algorithm and understanding effects of particle nonsphericity and refractive index errors on the size distribution retrieval from multispectral optical depth. In section 2, we present a new retrieval algorithm. This algorithm includes a regularization algorithm that considers the smoothness constraint as well as the nonnegativity constraint and an objective method for choosing the Lagrange multiplier controlling the degree of the smoothness artificially imposed on the desired size distribution. In section 3, the new retrieval algorithm is evaluated by comparing with an iterative algorithm and the method of singular value decomposition. In section 4, the effect of particle nonsphericity on size distribution retrieval is systematically investigated by taking the advantages of the recent developments in calculating single scattering by nonspherical particles. Both the Mie theory and the recently developed ADT for finite cylinders are used. The effect of refractive index errors is investigated using three available refractive index data sets for water in section 5. A further examination of the retrieval process is made in section 6. The results are summarized in section 7.

2. New Algorithm for Size Distribution Retrieval

2.1. Background

Optical remote sensing has been increasingly used to measure size distributions in scientific research and industrial technologies, including multispectral extinction measurements [*Arnott et al*., 1997], multispectral backscattering measurements [*Ben-David and Herman*, 1985], and multiangular scattering measurements [*Heintzerberg*, 1978]. Despite the subtle differences, most remote sensing techniques require solving a Fredholm integral equation of the first kind [*Twomey*, 1977]. Take the inversion of multispectral extinction measurements as an example, along with the assumption of single scattering. The optical depth (b) of a particulate cloud can be expressed as

$$\int_{D_{\min}}^{D_{\max}} K(y, D)x(D)\, dD = b(y), \tag{1a}$$

$$K(y, D) = LC_e(y, D), \tag{1b}$$

where y represents the wavenumber of the electromagnetic wave, D is the particle diameter, $D_{\min}$ and $D_{\max}$ are the smallest and largest diameter, respectively, $x(D)$ is the size distribution, $C_e(D, y)$ is the extinction cross section of a particle with diameter D at wavenumber y, and L is the physical path. Note that the dependence of $C_e(D, y)$ on the complex refractive index $m = m_r - im_i$ is implicitly included in the wavenumber dependence. Given L, D, y, and m, the kernel function $K(y, D)$ can be calculated on the basis of a suitable light-scattering theory, such as the Mie theory for homogeneous spheres. The angular-scattering technique yields a similar equation. In this case, one measures the scattering intensities at various scattering angles.

In practice, one needs to discretize (1) in order to solve it numerically because signals are practically measured at only a finite number (M) of variable y and the integral equation cannot generally be solved analytically. Without loss of the generality the discrete version of (1) is described by the matrix equation

$$\mathbf{Ax} = \mathbf{b}, \tag{2}$$

where $\mathbf{A}$ is an $M \times N$ base matrix with the component $A_{ij} = \Delta D \int_{D_j}^{D_j+\Delta D/2} K(\gamma_i, D)\, dD$, $\mathbf{x}$ is an $N \times 1$ vector whose component x_j represents the particle concentration at $D = D_j$, $\mathbf{b}$ is an $M \times 1$ vector whose component b_i is the measured signal at y_i.

2.2. Ill-Posedness and Solution Ambiguity

A cursory examination of (2) may lead one to consider that the size distribution retrieval is trivial because standard methods are available to solve (2) [*Lawson and Hanson*, 1995]. This is true when the base matrix $\mathbf{A}$ is well conditioned. Unfortunately, this is not true for our problem. The primary difficulty lies in the notorious ill-posedness carried over from the original integral equation. The ill-posedness is often characterized by a condition number of $\mathbf{A}$ much larger than 1. To demonstrate the ill-posedness of retrieving size distribution from multispectral optical depth measurements, the singular value decomposition (SVD) analysis of a base matrix $\mathbf{A}$ is made (see the Appendix about SVD). The base matrix $\mathbf{A}$ is generated by applying Mie theory to ice spheres with $M = 289$ and $N = 129$ (number of wavenumbers and size bins, respectively). The refractive index is from *Warren* [1984]. Figure 1 shows the distribution of singular values (solid curve). The dashed curve shows the truncated condition number defined as ratio of the largest singular value to the singular value corresponding to the index of singular value, or the condition number at the corresponding truncation level; the highest value on this curve

is the condition number. The condition number of this specific problem is about 10^{13}, indicating that the retrieval is severely ill-posed.

The ill-posedness will cause the ambiguity of retrieved size distributions: an infinite number of size distributions may satisfy the optical depth measurements to acceptable accuracy. To demonstrate the solution ambiguity associated with the ill-posedness, size distribution retrieval is made using the standard least squares method that does not use any additional constraints, and using SCNNLS, a new algorithm that uses both smoothness and nonnegativity constraint (as described in section 2.3). The synthetic spectral optical depths are generated by applying the above matrix **A** to a given size distribution. The results are shown in Figure 2. As shown in Figure 2a, the two methods yield totally different size distributions. A naive application of the standard least squares method produces a solution (dotted curve; note the different units and negative values!) that is far from the true size distribution (solid curve). The SCNNLS algorithm yields a solution (dashed curve) close to the true size distribution. However, as shown in Figure 2b, despite the significant differences between retrieved size distributions, the synthetic optical depths calculated from both retrieved size distributions all fall close to the true one, suggesting that solution ambiguity exists, and it is misleading to choose the retrieved size distribution only based on the agreement between measured optical depth and that calculated from the retrievals. It is noteworthy that no random errors are added to the optical depth, suggesting that the problem of retrieving size distributions from multispectral optical depth measurements is so seriously ill-posed that the computational errors alone (e.g., round-off errors) can cause serious problems.

2.3. New Regularization Method

As demonstrated above, serious ill-posedness and the associated solution ambiguity occur in retrieving size distribution from multispectral optical depth measurements. A common exercise to suppress the ill-posedness is to stabilize the problem by imposing additional conditions (constraints) on the desired size distribution to reduce the function space in which the solution lies. Such processes and methods of stabilizing the ill-posed problem are generally called regularization, and the reasonable solution thus found is called the regularized solution [*Twomey*, 1977; *Tikhonov and Arsenin*, 1977; *Hansen*, 1998]. The most commonly used constraints are nonnegativity and smoothness.

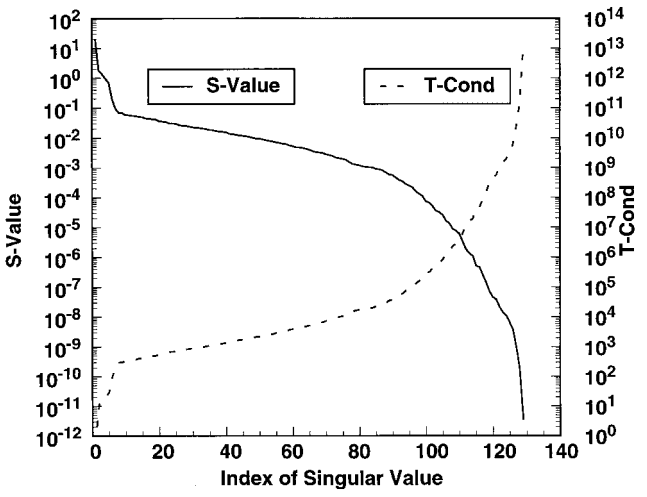

Figure 1. Singular values (S-value) and truncated condition number (T-cond) of the matrix **A**. It shows that the singular values decrease to about 10^{-12} continuously with the index of singular value and that the truncated conditions increase up to about 10^{-13}, the condition number of the matrix **A**. See the text for relevant definitions.

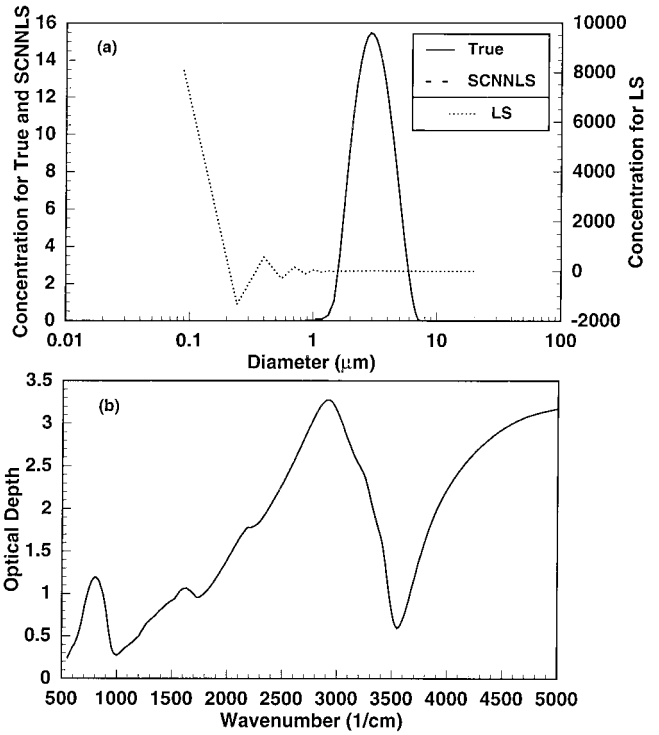

Figure 2. An example that shows the solution ambiguity due to the ill-posedness. The same base ill-conditioned matrix as shown in Figure 1 is used in the retrieval. In Figure 2a, the agreement between the true and the SCNNLS-retrieved size distribution is so good that they almost overlap into a curve. The same is true for the agreement between the true and the retrieved optical depths as shown in Figure 2b. The same legend is used for Figures 2a and 2b.

A natural way to combine the smoothness constraint with the original equation was introduced independently by *Phillips* [1962] and *Tikhonov* [1963], and some modifications of Phillips' work was suggested by *Twomey* [1963]. Briefly, with a Lagrange multiplier λ the constrained least squares problem becomes

$$\min_{x} \left(\|\mathbf{Ax} - \mathbf{b}\|^2 + \lambda\|\mathbf{Lx}\|^2\right), \tag{3}$$

where **L** is a $P \times N$ smoothing matrix with $P \times N$ that is usually a discrete representation of a differential operator. It is noteworthy that researchers in different fields use different names to represent this algorithm. Atmospheric scientists tend to call this algorithm "Philip-Twomey algorithm" while "Tikhonov algorithm" is more common to mathematicians. In this paper the name PTT algorithm is used to represent this method. The PTT algorithm has found wide applications [e.g., *Steele and Turco*, 1997]. However, a direct use of the PTT algorithm may lead to negative values. The problem of "negative values" has been frustrating researchers for a long time.

Obtaining a nonnegative solution (if possible at all) often involves tedious procedures. This is better illustrated by a paragraph in the work of *Steele and Turco* [1997]: " .... Since excessively large values of λ are sometimes necessary to force the values of $x(D)$ to be positive at all grid points (diameters) simultaneously, solutions for smaller values of λ must often be modified by replacing any negative values with positive but small ones. When physical solutions cannot be found, we use the solution from the initial inversion to modify the weighting function for subsequent inversions ...." Also, it is worth mentioning that a very large λ will give an oversmoothed solution.

On the other hand, to obtain a nonnegative solution, *Lawson and Hanson* [1974] (see the second edition in 1995) developed an algorithm to solve a nonnegative least squares problem (NNLS):

$$\min_{x} (\|\mathbf{Ax}-\mathbf{b}\|^2), \text{ subject to } \mathbf{x} \geq \mathbf{0}. \tag{4}$$

This method has received some applications in size distribution measurements. For example, *Hagen and Alofs* [1983] applied it to measure aerosol size distributions from mobility measurements. *Kim and Boatman* [1990] used it to modify droplet size distributions measured with an FSSP probe. Although the NNLS guarantees a nonnegative solution, the solution may have unrealistic fluctuations and spikes when the inverse problem is seriously ill-posed, such as retrieving size distributions from multispectral optical depth measurements.

The shortcomings of PTT and NNLS can be circumvented by coupling both together in two steps. First, the minimization problem of (3) is equivalent to solving the corresponding normal equation

$$(\mathbf{A}^t\mathbf{A} + \lambda\mathbf{L}^t\mathbf{L})\mathbf{x} = \mathbf{A}^t\mathbf{b}, \tag{5}$$

where the superscript "t" indicates the matrix transpose. See *Twomey* [1977] or *Liu* [1998] for the derivation of (5). Second, applying NNLS to (5) yields a smoothed nonnegative solution. This new algorithm is named the smoothing-constrained NNLS and is denoted by SCNNLS. This method overcomes the disadvantages of more-than-one regularization parameters and slowness of the iterative method and that of lacking nonnegativity constraint in the TSVD.

2.4. *L*-Curve Method for Choosing the Lagrange Multiplier

The nonnegativity constraint is physically realistic because particle number concentration cannot be negative. However, the smoothness constraint needs to be used with caution. Size distributions of various smoothness may occur in the atmosphere, depending on the physical processes and scales involved [*Liu and Hallett*, 1998; *Liu*, 1998]. Therefore finding an optimal Lagrange multiplier is as important as the algorithm itself. A very large multiplier leaves out information available in the measurement, while a very small multiplier produces a solution significantly contaminated by errors. Furthermore, the optimal multiplier depends on measurement errors, properties of the base matrix **A**, and the smoothness of the desired size distribution. In reality, all these things are seldom known in advance. Therefore an objective approach that does not require such preinformation is desirable for choosing Lagrange multiplier.

The method of the L curve was proposed by mathematicians in the 1970s [*Hansen*, 1998] to find the optimal Lagrange multiplier in PTT or particularly the special case with **L** being an identity matrix. The method has received increasing attention recently [*Hansen*, 1998]. For PTT the L curve is a plot of $\|\mathbf{Ax-b}\|$ versus $\|\mathbf{Lx}\|$ [*Hansen*, 1998]. $\|\mathbf{Ax-b}\|$ is the residue error in original matrix equation. $\|\mathbf{Lx}\|$ is a measure of size distribution smoothness; a smaller value indicates more smoothness. For TSVD the L curve is the plot of $\|\mathbf{Ax-b}\|$ versus $\|\mathbf{x}\|$. It has been proven that for PTT and its special case TSVD, a plot of residual norm $\|\mathbf{Ax-b}\|$ versus $\|\mathbf{Lx}\|$ exhibits a clear corner [*Hansen*, 1998]. In fact, the name of "L curve" comes from the fact that the curve of $\|\mathbf{Ax-b}\|$ versus $\|\mathbf{Lx}\|$ has an L-shaped corner as shown in Figures 3 and 4. Therefore the L curve can be understood as a curve characterizing the relationship between the solution smoothness and the residue error, with the regularization parameter, corresponding to the corner of the L curve, gives an optimal tradeoff between the imposed smoothness and the residue error. It is only recently that the L-curve method has been applied to size distribution measurements [*Ramachandran et al.*, 1996] and atmospheric remote sensing [*Schimpf and Schreier*, 1997].

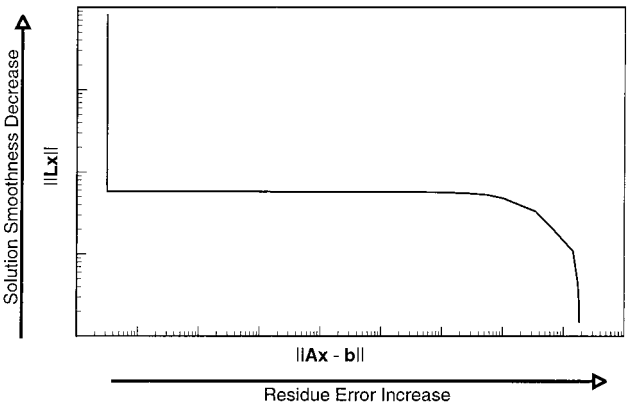

Figure 3. A conceptual representation of the L curve.

However, applications to inverse problems constrained by smoothness as well as nonnegativity have not been reported. A number of numerical studies have been made to verify the applicability of the "L-curve" idea to SCNNLS. An example of the L curve for SCNNLS is shown in Figure 4. Also shown in Figure 4 is the relationship between the relative size distribution error $r_x = \|\mathbf{x} - \mathbf{x}^*\|/\|\mathbf{x}^*\|$ ($\mathbf{x}^*$ and $\mathbf{x}$ are the true and retrieved size distributions) and the residue error (pluses). Figure 4 indicates that the λ corresponding to the corner of the

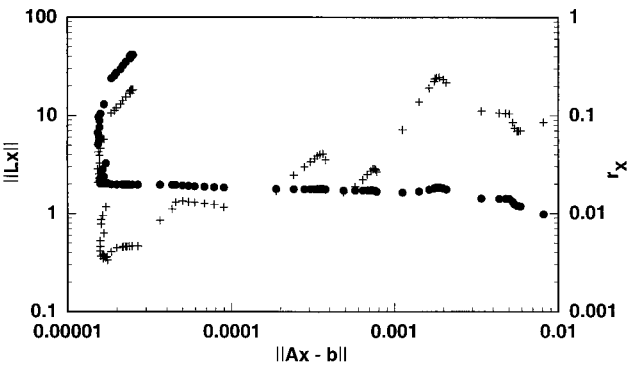

Figure 4. An example of the L curve when applying SCNNLS to the size distribution retrieval. Values of r_x are the plus symbols.

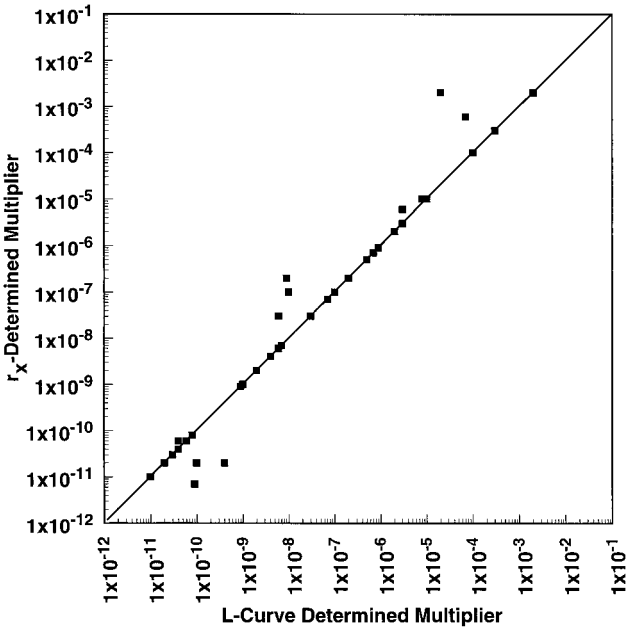

Figure 5. An example showing that the Lagrange multipliers determined by the L curve method almost yield the best retrieval.

L curve gives the best size distribution retrieval (lowest r_x). Figure 5 further shows the relationship between the λ determined by use of the L-curve method and that determined on the basis of the relative size distribution error. These results show that although the "L corner" may not be so sharp as that in PTT, depending on the specific problem, a λ that gives an optimal trade-off between the imposed smoothness and the residue error can still be located.

3. Evaluation of the SCNNLS Algorithm

To evaluate SCNNLS, numerical studies are made for spherical particles. The Mie theory and the refractive indices for ice [*Warren*, 1984] are used to generate the base matrix **A** and a synthetic multispectral optical depth for a given size distribution. Then a corresponding size distribution is retrieved by inverting the synthetic optical depth. To demonstrate the advantages of the new procedure, size distribution retrievals are also made for the same data set by use of the iterative algorithm presented by *Arnott et al*. [1997] and the method of truncated singular value decomposition (TSVD) (see the Appendix). Figure 6 is an example of the retrieval for a smooth size distribution. It can be seen from these figures that the size distributions retrieved by all the three methods are sufficiently good to the human eye in terms of the size distribution as well as the optical depth. The agreements are so good that the curves corresponding to different retrieval algorithms all overlap with the true values. However, the iterative algorithm is much slower than the other two. Another disadvantage of the iterative algorithm is that its performance depends on two parameters: smoothing factor and iteration level. The TVSD is as fast as SCNNLS. However, a careful examination of the zoom-in plots for the end of small particles marked by 1 and the end of large particles marked by 2 reveals that TSVD produces unrealistic negative concentrations, particularly at both ends of particle sizes. These results demonstrate that

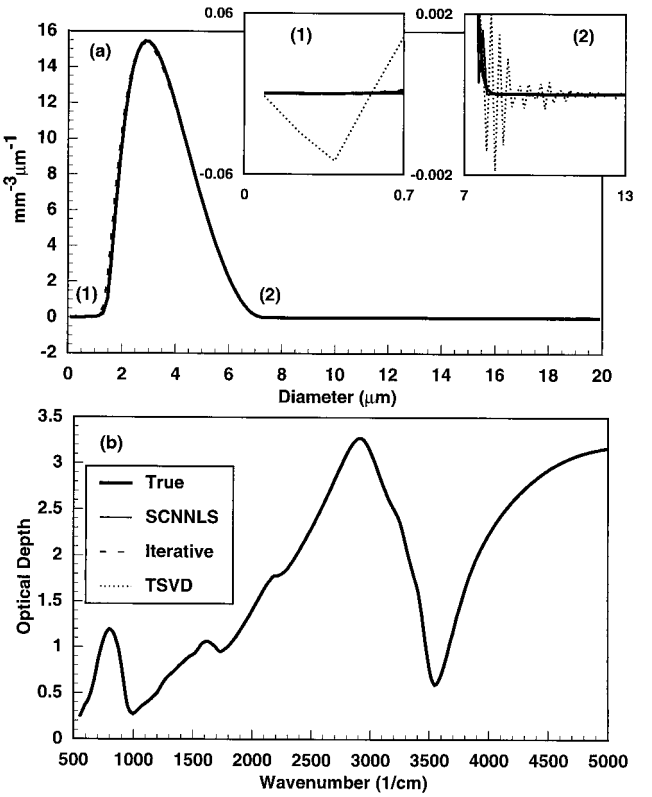

Figure 6. (a) Size distribution retrieval and (b) the corresponding optical depth. The thick solid curves represent the true size distribution and the true optical depth. The thin solid curves represent the size distribution retrieved from SCNNLS and the optical depth calculated from this size distribution. The dashed curves represent the size distribution retrieved from the iterative algorithm and the optical depth calculated from this size distribution. The dotted curves represent the size distribution retrieved from TSVD and the optical depth calculated from this size distribution.

SCNNLS outperforms the other two algorithms, as summarized in Table 1. In the following sections, SCNNLS will be used to investigate the effects of particle nonsphericity and refractive index errors on size distribution retrievals.

4. Influences of Particle Nonsphericity

4.1. Mie Theory Approximation

The Mie theory has been extensively used in optically sizing instruments for measuring size distributions. When nonspherical particles exist, size distribution measurements with Mie-theory-based instruments are expected to have distortions. Because it is difficult and expensive to compute scattering

Table 1. Comparison of Different Retrieval Algorithms

Features	SCNNLS	TSVD	Iterative
Smoothness constraint	yes	yes	yes
Nonnegativity constraint	yes	no	yes
Choose regularization factor	yes	yes	no*
Computational speed	fast	fast	slow

*Iterative algorithm has two regularization parameters to be determined.

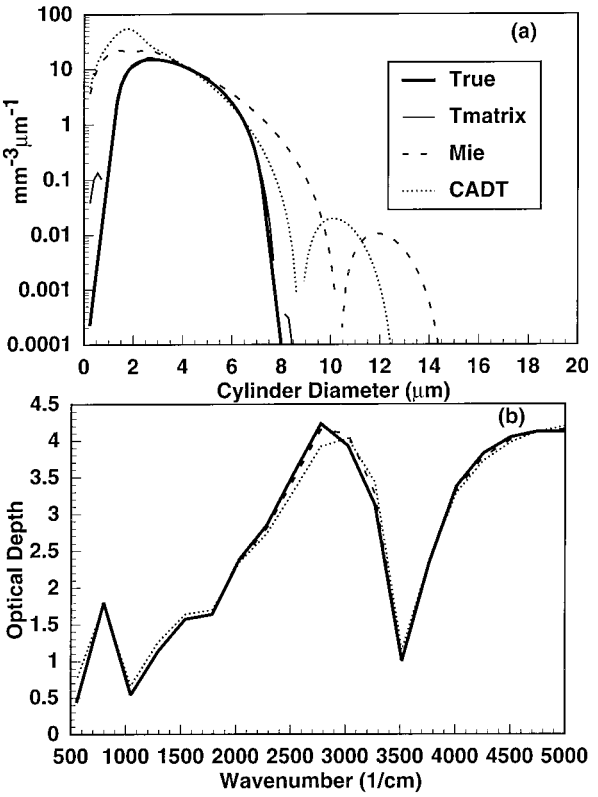

Figure 7. Influence of applying Mie theory (dashed curves) and CADT (dotted curves) to the retrieval of size distribution of finite cylinders with aspect ratio $D/L = 1.0$: (a) size distributions, (b) corresponding optical depths. The same legend is used for Figures 7a and 7b. Note that when the exact light-scattering method (**T** matrix) is used, the retrieved size distribution (Figure 7a) and optical depth (Figure 7b) are so good that they almost overlap with the true values.

properties for nonspherical particles, only a few studies have tried to address the influence of particle nonsphericity, to a limited extent. *Heintzenberg* [1978] investigated the error of applying the Mie theory to retrieving size distributions of nonspherical particles from multiangle-scattering experiments. The scattering intensities in his study were generated by combining known size distributions with previous experimental results for various nonspherical particles. He found (1) both spurious smaller and larger spheres, (2) much higher particle concentration, and (3) a second mode for large particles.

Recently, the T-matrix method for nonspherical scattering has been significantly improved [*Mishchenko et al*., 1996]. To study the influence of particle nonsphericity, the T-matrix method is used to generate the base matrix **A** and synthetic spectral optical depth for given size distributions of finite cylinders. The synthetic optical depth is then inverted by use of both the T-matrix-calculated **A** and that calculated on the basis of the Mie theory for spheres. It is noteworthy that even the T-matrix method is still so computationally intensive ("M times N" T-matrix calculations are needed to generate a $M \times N$ base matrix **A**) that the matrix **A** has been generated only for cylinders with the diameter-to-length (aspect ratio) = 1.0 and $M = 19$; $N = 129$. The values of $M = 19$ and $N = 129$ are not optimal; they are the results of the compromise between retrieval performance, size resolution, and available computer resources. (Based on some numerical evaluation, an optimal choice that minimizes the normalized residue would be $M \approx N$ [see *Liu*, 1998].) As shown in Figure 7a, when the appropriate scattering theory (here T-matrix method) is used, the retrieved size distributions (thin solid curve) agree well with the true size distribution (thick solid curve). However, when Mie theory is used, the retrieved size distribution (dotted curve) significantly departs from the true size distribution. Spurious particles are generated at both size ends, and a spurious second mode of large particles occurs. Despite the significant differences in retrieved size distributions, only small deviations occur for retrieved optical depths.

4.2. ADT Approximation

The anomalous diffraction theory (ADT) is another common approximation to scattering by nonspherical particles. A number of retrieval schemes have been developed on the basis of the ADT for spheres [*Box and McKellar*, 1978; *Klett*, 1984]. Applying the ADT for spheres to spherical droplets, *Arnott et al*. [1997] found that ADT gave a worse size distribution retrieval as well as a worse agreement between modeled and measured optical depths compared to the Mie theory. Recently, the ADT for finite cylinders (CADT) has been developed [*Liu et al*., 1998]. To study the performance of ADT for nonspherical particles, CADT is used to generate the base matrix **A**, which is then used to invert the same synthetic optical depth data as those used for Mie theory. As shown in Figure 7, similar to the Mie theory approximation, CADT also produces spurious particles. CADT is worse for small particles than Mie theory. This may be due to the large extinction overestimation of ADT when particles are small.

5. Effects of Refractive Index Errors

So far, refractive indices are assumed to be accurately known in the size distribution retrieval. In reality, our knowledge of refractive index, however, is uncertain. For aerosols, refractive index is essentially unknown since atmospheric aerosols are mixtures of a variety of aerosol types and chemical compositions (e.g., sulfate, nitrate, ammonium, condensed organic species, elemental or black carbon, and mineral dust) [*Penner et al*., 1994]. Figure 8 shows the three widely used refractive index data sets for water, suggesting that uncertainties exist even for the well-documented water refractive index, particularly for the real part around the Christiansen band where the real part is closest to unity. Such uncertainties are expected to have some effect on the size distribution retrieval.

More research has been performed on the effect of uncertain refractive index than on the effect of particle shape. *Shifrin and Gashko* [1974] examined the size distributions inverted by the statistical regularization method from angular scattering when the incorrect value of the refractive index was assumed. They first generated a theoretical angular-scattering function using a known size distribution and $m = 1.33$ and then performed size distribution retrievals using kernels generated with nine different refractive indices: $m = 1.15 - 0.00i$, $1.25 - 0.05i$, $1.29 - 0.05i$, $1.3 - 0.1i$, $1.31 - 0.00004i$, $1.33 - 0.0i$, $1.353 - 0.006i$, $1.4 - 0.05i$, and $1.5 - 0.06i$. They found that the size distribution retrieval is very sensitive to the refractive index, being more sensitive to the imaginary part than to the real part of the index. Unfortunately, it is not clear whether the Mie theory or ADT was used in their calculation. *Twitty* [1975] studied the sensitivity to refractive index of inverting solar aureole measurements. The inversion method he

used was a nonlinear iterative method originally proposed by *Chahine* [1968]. A spline fit of a size distribution measured by impactor methods and $m = 1.54$ were used to generate theoretical phase functions at 20 scattering angles between 1° and 20° based on the Mie theory. He estimated the effect of refractive index by changing $m = 1.54$ to 1.33, and found that the incorrect index gave a poor retrieved size distribution in the range of small particles (radii < 1 μm). *King et al.* [1978] retrieved size distributions from optical depths. The Mie theory and $m = 1.54$ were used to generate the kernel and synthetic optical depth discretized with eight wavelengths between approximately 0.4 and 1.03 μm. The effect of refractive index on size distribution retrieval was investigated by using $m = 1.45$ and $1.45 - 0.03i$. *Santer and Herman* [1983] studied the effect of refractive index on size distribution retrieval from forward scattering using the diffraction approximation and the Chahine iterative scheme. They used $m = 1.33$, 1.45, and 1.55 and found that a correct m is important in the range of small particles. The wavelength they used was 1 μm.

These studies are limited for wavelength-independent refractive indices. To demonstrate the effect of small errors in wavelength-dependent refractive indices, size distributions of spherical particles are retrieved using the three different published data sets of refractive index for liquid water shown in Figure 8. The retrieval procedures are as follows: First, given the true size distribution (thick solid curve in Figure 9a), the refractive indices by *Downing and Williams* [1975] are used to generate a "true optical depth" (thick solid curve in Figure 9b). Then the retrievals are made using the base matrices generated by use of the three different sets of refractive index. Figure 9 shows the retrieval results, suggesting that a perturbation of refractive index as small as that between the three commonly used data sets for liquid water can cause serious retrieval errors, particularly at the end of small particles. In the atmosphere the refractive indices for both aerosols and ice crystals are likely more uncertain than this example; the effect of refractive index errors is therefore expected to be larger.

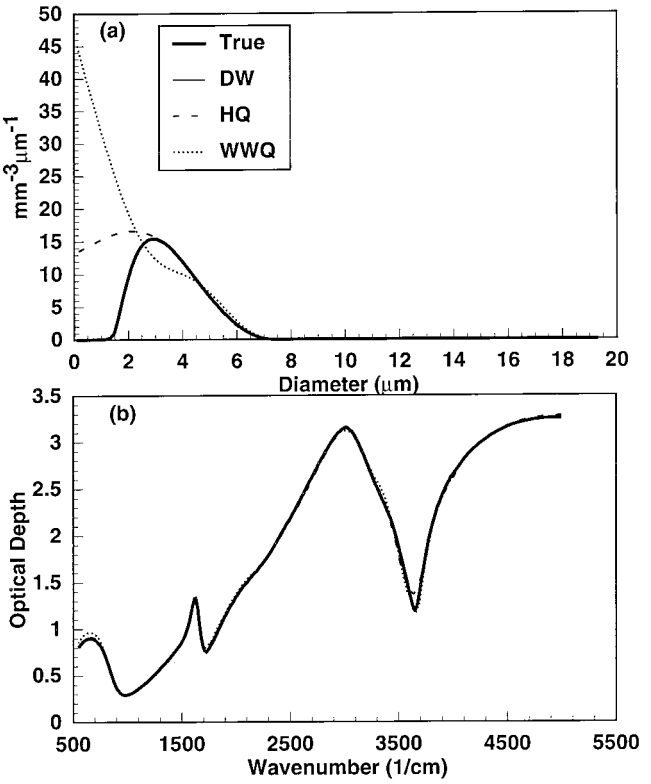

Figure 9. Effects of refractive index errors on size distribution retrieval: (a) retrieved size distributions using different index sets, (b) corresponding optical depths. The same legend is used for Figures 9a and 9b. The DW results overlap almost perfectly with the true curves.

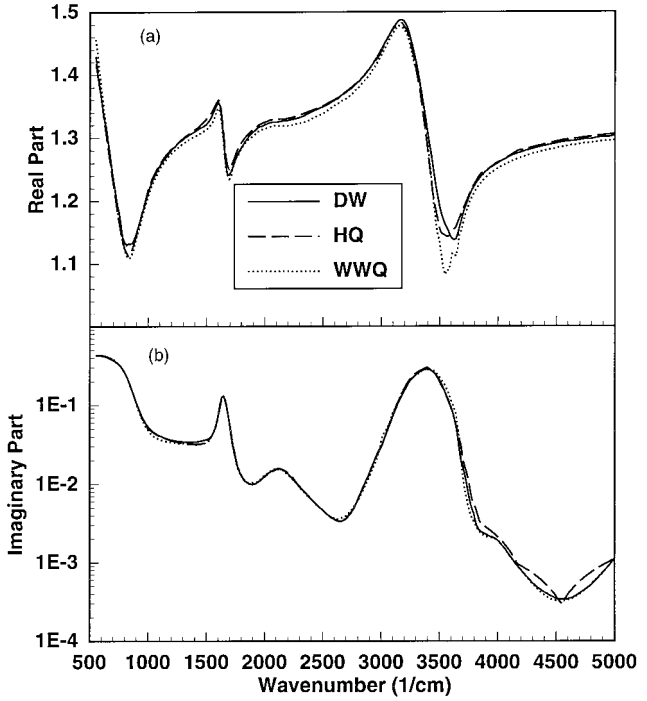

Figure 8. Three published refractive index data sets for liquid water: (a) change of the real part of refractive index with wavenumber, (b) change of the imaginary part with wavenumber. DW is *Downing and Williams* [1975]; HQ is *Hale and Querry* [1973]; WWQ is *Wieliczka et al.* [1989].

6. Discussion

Section 4 demonstrates that severe distortions occur when either the Mie theory or the ADT for finite cylinders is used to retrieve size distributions of finite cylinders. Section 5 demonstrates that incorrect refractive indices also cause significant distortions of retrieved size distributions for spherical particles. A further examination reveals that either applying an approximate light-scattering theory (Mie theory or ADT) to nonspherical particles or using incorrect refractive indices results in systematic errors in the base matrix **A**. It is such systematic errors in **A** which conspire with the ill-posedness to cause the distortions of retrieved size distributions. The retrieval process actually transforms the errors in the matrix **A** into the error in retrieved size distribution, yet makes the agreement between true and retrieved optical depths reasonably better.

The effects of retrieval can be studied by comparing optical depths calculated from the true size distribution and the retrieved size distribution. As illustrations, Figure 10 shows the differences between the true and the calculated optical depths when the T-matrix method and the Mie theory are applied to

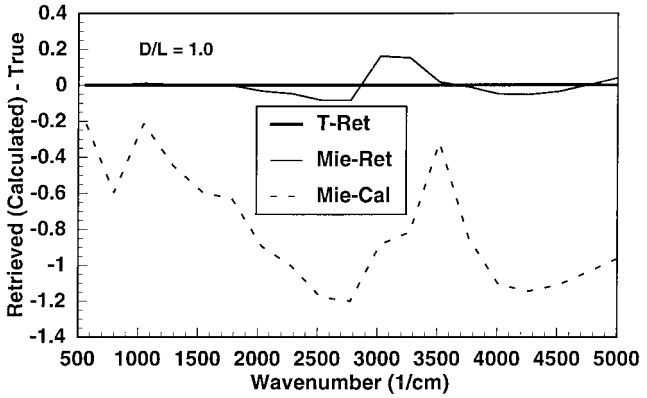

Figure 10. An example showing that retrieval processes tend to improve the agreement between the true optical depth and that calculated from the retrieved size distribution by transforming the errors in the base matrix **A** (or model errors) into the error in retrieved size distributions.

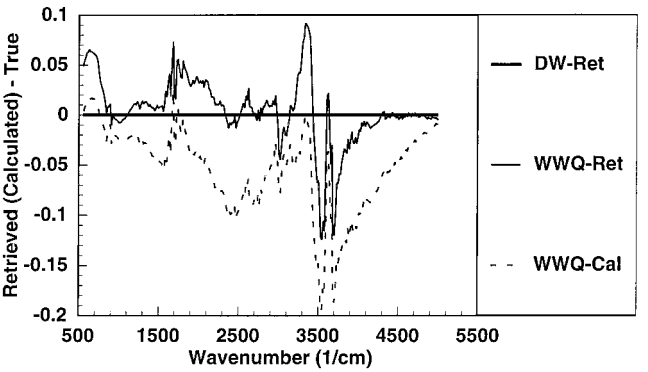

Figure 11. An example showing that retrieval processes tend to improve the agreement between the true optical depth and that calculated from the retrieved size distribution by transforming the errors in the base matrix **A** (or model errors) into the error in retrieved size distributions.

finite cylinders. Figure 11 shows the differences between the true and the calculated optical depths when different sets of refractive index are used to retrieve size distributions of spherical particles. The WWQ refractive index set is chosen because its deviation from the DW set is larger than that of the HQ set. As expected, for both cases, the difference between the true optical depth and that calculated from the retrieved size distribution is generally smaller than that between the true optical depth and the optical depth calculated from the true size distribution.

Previous studies have been focused on the effect of measurement errors on size distribution retrieval [*Twomey*, 1977]. The studies here suggest that the effect of model errors on the size distribution retrieval is at least equally important, if not more important in the atmosphere because of the existence of nonspherical particles and the uncertainties in the refractive indices. The results also suggest caution in interpreting size distributions measured by Mie-theory-based instruments when nonspherical particles and/or errors in refractive index exist.

7. Concluding Remarks

The ill-posedness and the associated solution ambiguity of retrieving size distributions from multispectral optical depth measurements are discussed and demonstrated by means of singular value decomposition. A new retrieval algorithm SCNNLS is presented and compared with an iterative algorithm and the method of truncated singular value decomposition. The SCNNLS incorporates smoothness and nonnegativity into the algorithm with the L-curve method to choose the optimal Lagrange multiplier. The results suggest that the new SCNNLS outperforms the other two algorithms.

The influence of particle nonsphericity on size distribution retrieval was studied by using the T-matrix method to calculate extinction cross sections of finite cylinders and then inverting the optical depth by use of the base matrix **A** calculated on the basis of the T-matrix method, the Mie theory, and the ADT for finite cylinders developed. The results show that severe distortions of retrieved size distributions occur when either applying the Mie theory or the ADT to nonspherical particles. Retrieval distortions are also found when incorrect refractive indices are used. The effects on size distribution retrieval of particle nonsphericity and refractive index errors have one thing in common: they are all model errors that cause systematic errors in the base matrix **A**. Further analysis reveals that the retrieval processes produce a better agreement between true optical depth and that calculated from the retrieved size distribution, at the cost of making worse the agreement between the true and the retrieved size distribution. These results suggest that caution should be applied in analyzing and interpreting size distributions measured in the presence of nonspherical particles and/or potential refractive index errors.

It is noteworthy that although this work is specifically concerned with retrieving size distributions from multispectral optical depth measurements, the retrieval algorithms presented in here have many potential applications because most in situ instruments for detecting size distributions also require solutions of similar inverse problems. Examples cover most commonly used instruments for measuring particles from very small nanometer particles to large precipitation particles, including the technique of pulse height analysis for measuring nanometer particles [*Weber et al*., 1998], the screen-type diffusion battery [*Maher and Laird*, 1985], differential mobility analyzer [*Hagen and Alofs*, 1983], nuclepore filter sampler [*Melo and Philips*, 1974], cascade and variable-slit impactors [*Cooper and Spielman*, 1976], in situ light-scattering optical counters such as the FSSP probe [*Jaenicke*, 1972; *Baumgardner and Spowart*, 1990], and the PMS-optical array probes for measuring large cloud particles and precipitation particles [*Korolev et al*., 1998]. *Preining* [1966] offered a general discussion on the instrumentation for measuring size distributions and defined the mutual influence among particles of different sizes as cross sensitivity. It is obvious that the concept of cross sensitivity is closely related to the ill-posedness of the problem.

Appendix: Singular Value Decomposition, Ill-Posedness and TSVD

Consider the discrete version described by (2). Using the generalized inverse theory, the solution can be expressed as

$$\mathbf{x} = \mathbf{A}^{+}\mathbf{b}, \tag{A1}$$

where $\mathbf{A}^{+}$ is the generalized inverse of **A** [*Israel and Greville*, 1974]. If **b** is perturbed by $\Delta\mathbf{b}$, then the perturbed solution "$\mathbf{x} + \Delta\mathbf{x}$" satisfies

$$\mathbf{A}(\mathbf{x} + \Delta\mathbf{x}) = \mathbf{b} + \Delta\mathbf{b}. \tag{A2}$$

The solution perturbation is given by

$$\Delta\mathbf{x} = \mathbf{A}^{+}\Delta\mathbf{b}. \tag{A3}$$

Taking norms of both sides of (6) gives

$$\|\Delta\mathbf{x}\| \le \|\mathbf{A}^{+}\|\|\Delta\mathbf{b}\|. \tag{A4}$$

Here $\|\mathbf{w}\|$ represents the Euclidean norm when $\mathbf{w}$ is a vector and a matrix norm when $\mathbf{w}$ is a matrix. Details about various norms are referred to *Lawson and Hanson* [1995]. From $\|\mathbf{b}\| \le \|\mathbf{A}\|\,\|\mathbf{x}\|$, we have

$$\|\mathbf{x}\| \ge \frac{\|\mathbf{b}\|}{\|\mathbf{A}\|}. \tag{A5}$$

A combination of (A4) and (A5) yields

$$\frac{\|\Delta\mathbf{x}\|}{\|\mathbf{x}\|} \le \text{cond}\,\frac{\|\Delta\mathbf{b}\|}{\|\mathbf{b}\|}, \tag{A6}$$

where cond $= \|\mathbf{A}\|\,\|\mathbf{A}^{+}\|$ is the condition number of $\mathbf{A}$.

Equation (A6) indicates that a small error in $\mathbf{b}$ will cause a large error in the solution when cond $\gg 1$. A matrix $\mathbf{A}$ with a large condition number is called ill conditioned. Therefore the condition number characterizes the degree of the ill-posedness of the problem.

The ill-posedness of the problem can be further understood by means of the singular value decomposition (SVD) of the matrix $\mathbf{A}$. The SVD of $\mathbf{A}$ is given by

$$\mathbf{A} = \mathbf{U}\mathbf{S}\mathbf{V}^{t} = \sum_{i}^{r} \mathbf{s}_i\mathbf{u}_i\mathbf{v}_i^{t}, \tag{A7}$$

where $\mathbf{U} = [\mathbf{u}_1, \mathbf{u}_2, \ldots, \mathbf{u}_n] \in R^{m\times n}$ is an orthogonal matrix with the left singular vector $\mathbf{u}_i$ $(i = 1, 2, \ldots, M)$ as its column vector, $\mathbf{V} = [\mathbf{v}_1, \mathbf{v}_2, \ldots, \mathbf{v}_n] \in R^{n\times n}$ is an orthogonal matrix with the right singular vector $\mathbf{v}_j$ $(j = 1, 2, \ldots, N)$ as its column vector, and $\mathbf{S}$ is an $M \times N$ diagonal matrix with $r \le \min(M, N)$ positive singular values σ_i ordered by magnitude, $\sigma_1 \ge \sigma_2 \ge \ldots \ge \sigma_r > 0$. Here r is the rank of the matrix $\mathbf{A}$. If the spectral norm of a matrix $\mathbf{A}$ is used, $\|\mathbf{A}\| = \max\{\|\mathbf{A}\mathbf{x}\|/\|\mathbf{x}\|\}$, then the following expressions hold [*Lawson and Hanson*, 1995]:

$$\|\mathbf{A}\| = \sigma_1 \tag{A8a}$$

$$\|\mathbf{A}^{+}\| = \sigma_r \tag{A8b}$$

$$\text{cond} = \frac{\sigma_1}{\sigma_r} \tag{A8c}$$

It is clear from (A8c) that a matrix $\mathbf{A}$ with small singular values has a large condition number, implying the problem is ill conditioned.

In addition to providing a tool for analyzing the ill-posedness of the problem, the singular value decomposition also provides a useful method for obtaining a regularized solution. Briefly, substituting (10) into (2), the solution is readily obtained as

$$\mathbf{x} = \sum_{i}^{r} \frac{g_i}{\sigma_i}\mathbf{v}_i, \tag{A9a}$$

$$g_i = \mathbf{u}_i^{T}\mathbf{b}, \tag{A9b}$$

$$\Delta\mathbf{x} = \sum_{i}^{r} \frac{u_i^{T}\Delta\mathbf{b}}{\sigma_i}\mathbf{v}_i. \tag{A9c}$$

These equations further indicate that if there is some errors in $\mathbf{b}$, the contributions of small values will contaminate the solution. Neglecting the contributions associated with small singular values, the solution is given by

$$\mathbf{x}^{(k)} = \sum_{i}^{k} \frac{g_i}{\sigma_i}\mathbf{v}_i. \tag{A10}$$

This method is called the truncated singular value decomposition (TSVD). It is obvious that the truncation level $k < r$ plays the role of regularization. The regularization is too strong if k is too small, while the solution is too sensitive to errors if k is too large. Similar to discretization, there is a tradeoff between the variance of the solution and the bias of the solution [*Marquardt*, 1970].

Acknowledgment. This work was supported by NSF grant ATM-9413437.

References

Arnott, W. P., Y. Liu, and J. Hallett, Unreasonable effectiveness of mimicking measured infrared extinction by hexagonal ice crystals with Mie ice spheres, in *Optical Remote Sensing of the Atmosphere*, *OSA Tech. Dig. Ser.*, vol. 5, pp. 216–218, Opt. Soc. of Am., Washington, D. C., 1996.

Arnott, W. P., C. Schmitt, Y. Liu, and J. Hallett, Droplet size spectra and water vapor concentration of laboratory water clouds: Inversion of FTIR (500–5000 cm^{-1}) optical depth measurement, *Appl. Opt.*, *36*, 5205–5216, 1997.

Baran, A. J., J. S. Foot, and D. L., Mitchell, Ice crystal absorption: A comparison between theory and implications for remote sensing, *Appl. Opt.*, *37*, 2207–2215, 1998.

Barber, P. W., and S. C. Hill, *Light Scattering by Particles: Computational Methods*, 261 pp., World Sci., River Edge, N. J., 1990.

Baumgardner, D., and M. Spowart, Evaluation of the forward scattering spectrometer probe, III, Time response and laser inhomogeneity limitations, *J. Atmos. Oceanic Technol.*, *7*, 666–672, 1990.

Ben-David, A., and B. M. Herman, Method for determining particle size distributions by nonlinear inversion of backscattered radiation, *Appl. Opt.*, *24*, 1037–1042, 1985.

Box, M. A., and B. H. J. McKellar, Analytic inversion of multispectral extinction data in the anomalous diffraction approximation, *Opt. Lett.*, *3*, 91–93, 1978.

Chahine, M. T., Determination of the temperature profile in an atmosphere from its outgoing radiance, *J. Opt. Soc. Am.*, *58*, 1634–1637, 1968.

Cooper, D. W., and L. A. Spielman, Data inversion using nonlinear programming with physical constraints: Aerosol size distribution measurements by impactors, *Atmos. Environ.*, *10*, 723–729, 1976.

Deirmendjian, D., A survey of light scattering techniques used in the remote monitoring of atmospheric aerosols, *Rev. Geophys.*, *18*, 341, 1980.

Downing, H. D., and D. Williams, Optical constants of water in the infrared, *J. Geophys. Res.*, *80*, 1656–1661, 1975.

Fu, Q., and K. N. Liou, Parameterization of the radiative properties of cirrus clouds, *J. Atmos. Sci.*, *50*, 2008–2025, 1993.

Hagen, D. E., and D. J. Alofs, Linear inversion method to obtain aerosol size distributions from measurements with a differential mobility analyzer, *Aerosol Sci. Technol.*, *2*, 465–475, 1983.

Hale, G. M., and M. R. Querry, Optical constants of water in the 200-nm to 200-μm wavelength region, *Appl. Opt.*, *12*, 555–563, 1973.

Hansen, P. C., *Rank-Deficient and Ill-posed problems: Numerical Aspects of Linear Inversion*, 247 pp., SIAM J. Appl. Math., Philadelphia, 1998.

Heintzenberg, J., Particle size distributions from scattering measure-

ments of nonspherical particles via Mie-theory, *Contrib. Atmos. Phys*., *51*, 91–99, 1978.
Israel, A., and T. N. E. Greville, *Generalized Inverses: Theory and Applications*, 395 pp., John Wiley, New York, 1974.
Jaenicke, R., The optical particle counter: Cross sensitivity and coincidence, *J. Aerosol Sci*., *30*, 95–111, 1972.
Kerker, M., Light scattering instrumentation for aerosol studies: An historical overview, *Aerosol Sci. Technol*., *27*, 522–540, 1997.
Kim, Y. J., and J. F. Boatman, Corrections for the effects of particle trajectory and beam intensity profile on the size spectra of atmospheric aerosols measured with a Forward Scattering Spectrometer Probe, *J. Atmos. Oceanic Technol*., *7*, 673–680, 1990.
King, M. D., D. M. Byrne, B. M. Herman, and J. A. Reagan, Aerosol size distributions obtained by inversion of special optical depth measurements, *J. Atmos. Sci*., *35*, 2153–2167, 1978.
Klett, J. D., Anomalous diffraction model for inversion of multispectral extinction data including absorption effects, *Appl. Opt*., *23*, 4499–4508, 1984.
Korolev, A. V., J. W. Strapp, and G. A. Isaac, Evaluation of the accuracy of PMS optical array probes, *J. Atmos. Oceanic Technol*., *15*, 708–720, 1998.
Lawson, C. L., and R. J. Hanson, *Solving Least Squares Problem*, 337 pp., SIAM, J. Appl. Math., Philadelphia, 1995.
Liu, Y., Size distribution of atmospheric particles: Scale-dependence, scattering properties of nonspherical particles and retrieval by inversion of spectral optical depth, Ph.D. dissertation, Univ. of Nevada, Reno, 1998.
Liu, Y., and J. Hallett, On size distributions of cloud droplets growing by condensation: A new conceptual model, *J. Atmos. Sci*., *55*, 527–536, 1998.
Liu, Y., W. P. Arnott, and J. Hallett, Anomalous diffraction theory for arbitrarily oriented finite circular cylinders and comparison with exact T-matrix results, *Appl. Opt*., *37*, 5019–5030, 1998.
Knollenberg, R. G., Techniques for probing cloud microstructure, in *Clouds, Their Formation, Optical Properties, and Effects,* edited by P. V. Hobbs and A. Deepak, pp. 15–91, 1981.
Maher, E. F., and N. M., Laird, EM algorithm reconstruction of particle size distributions from diffusion battery data, *J. Aerosol Sci*., *16*, 557–570, 1985.
Marquardt, D. W., Generalized inverses, ridge regression, biased linear estimation, and nonlinear estimation, *Technometrics*, *12*, 591–612, 1970.
Melo, C. T., and C. R. Phillips, Aerosol-size spectra by means of membrane filters, Theoretical study, *Environ. Sci. Technol*., *8*, 67–71, 1974.
Mishchenko, M. I., L. D. Travis, and D. W. Mackowski, T-matrix computations of light scattering by nonspherical particles: A review, *J. Quant. Spectrosc. Radiat. Transfer*, *55*, 535–575, 1996.
Mitchell, D. L., and W. P. Arnott, A model predicting the evolution of ice particle size spectra and radiative properties of cirrus clouds, II, Dependence of absorption and extinction on ice crystal morphology, *J. Atmos. Sci*., *51*, 817–832, 1994.
Penner, J. E., et al., Quantifying and minimizing uncertainty of climate forcing by anthropogenic aerosols, *Bull. Am. Meteorol. Soc*., *75*, 375–400, 1994.
Phillips, D. L., A technique for the numerical solution of certain integral equations of the first kind, *J. Assoc. Comput. Mach*., *9*, 84–97, 1962.
Preining, O., On the evaluation of aerosol size distributions, *J. Rech. Atmos*., *2*, 145–151, 1966.
Pruppacher, H. R., and J. A. Klett, *Microphysics of Clouds and Precipitation*, 954 pp., Kluwer Acad., Norwell, Mass., 1997.
Ramachandran, G., E. W. Johnson, and J. H. Vincent, Inversion techniques for personal cascade impactor data, *J. Aerosol Sci*., *27*, 1083–1097, 1996.
Santer, R., and M. Herman, Particle size distributions from forward scattered light using the Chahine inversion scheme, *Appl. Opt*., *22*, 2294–2301, 1983.
Schimpf, B., and F. Schreier, Robust and efficient inversion of vertical-sounding atmospheric high-resolution spectra by means of regularization, *J. Geophys. Res*., *102*, 16,037–16,055, 1997.
Shifrin, K. S., and V. A. Gashko, Reconstruction of the particle size distribution functions when the information about the refractive index of the particles is inexact, *Atmos. Oceanic Phys*., *10*, 943–949, 1974.
Steele, H. M., and R. P. Turco, Retrieval of aerosol size distributions from satellite extinction spectra using constrained linear inversion, *J. Geophys. Res*., *102*, 16,737–16,747, 1997.
Tikhonov, A. N., Solution of incorrectly formulated problems and the regularization method, *Sov. Math. Dokl*., *4*, 1035–1038, 1963.
Tikhonov, A. N., and V. Arsenin, *Solution of Ill-Posed Problems*, 224 pp., Winston and Sons, Washington, D. C., 1977.
Twitty, J. T., The inversion of aureole measurements to derive aerosol size distributions, *J. Atmos. Sci*., *32*, 584–591, 1975.
Twomey, S., On the numerical solution of Fredholm integral equations of the first kind by the inversion of the linear system produced by quadrature, *J. Assoc. Comput. Mach*., *10*, 97–101, 1963.
Twomey, S., *Introduction to the Mathematics of Inversion in Remote Sensing and Indirect Measurements*, 243 pp., Elsevier, New York, 1977.
Warren, S., Optical constants of ice from the ultraviolet to the microwave, *Appl. Opt*., *23*, 1206–1225, 1984.
Weber, R. J., et al., Inversion of ultrafine condensation nucleus counter pulse height distributions to obtain nanoparticle (~3–10 nm) size distributions, *J. Aerosol Sci*., *29*, 601–615, 1998.
Welch, R. M., S. K. Cox, and K. Y. Kondratyev, Determination of vertical profiles of aerosol size spectra from aircraft radiative flux measurements, 2, The effect of particle nonsphericity, *J. Geophys. Res*., *86*, 9795–9800, 1981.
Wieliczka, D. M., S. Weng, and M. R. Querry, Wedge-shaped cell for highly absorbent liquids: Infrared optical constants of water, *Appl. Opt*., *28*, 1714–1719, 1989.
Yang, P., K. N. Liou, and W. P. Arnott, Extinction efficiency and single-scattering albedo for laboratory and natural cirrus clouds, *J. Geophys. Res*., *102*, 21,825–21,835, 1997.

W. Patrick Arnott, J. Hallett, and Y. Liu (corresponding author), Desert Research Institute, Atmospheric Sciences Center, 5625 Fox Ave., Reno, NV 89506. (lyg@brl.gov)

(Received September 1, 1998; revised December 10, 1998; accepted December 17, 1998.)